

An Azophenine Radical-Bridged Fe₂ Single-Molecule Magnet with Record Magnetic Exchange Coupling

Ie-Rang Jeon,[†] Jesse G. Park,[†] Dianne J. Xiao,[‡] and T. David Harris*,[†][†]Department of Chemistry, Northwestern University, Evanston Illinois 60208-3113, United States[‡]Department of Chemistry, University of California, Berkeley, California 94720-1460, United States**S** Supporting Information

ABSTRACT: One-electron reduction of the complex [(TPyA)₂Fe^{II}(^{NPh}L²⁻)]²⁺ (TPyA = tris(2-pyridylmethyl)-amine, ^{NPh}LH₂ = azophenine = N,N',N'',N'''-tetraphenyl-2,5-diamino-1,4-diiminobenzoquinone) affords the complex [(TPyA)₂Fe^{II}(^{NPh}L^{3-•})]⁺. X-ray diffraction and Mössbauer spectroscopy confirm that the reduction occurs on ^{NPh}L²⁻ to give an *S* = 1/2 radical bridging ligand. Dc magnetic susceptibility measurements demonstrate the presence of extremely strong direct antiferromagnetic exchange between *S* = 2 Fe^{II} centers and ^{NPh}L^{3-•} in the reduced complex, giving an *S* = 7/2 ground state with an estimated coupling constant magnitude of $|J| \geq 900 \text{ cm}^{-1}$. Mössbauer spectroscopy and ac magnetic susceptibility reveal that this complex behaves as a single-molecule magnet with a spin relaxation barrier of $U_{\text{eff}} = 50(1) \text{ cm}^{-1}$. To our knowledge, this complex exhibits by far the strongest magnetic exchange coupling ever to be observed in a single-molecule magnet.

Over the past two decades, a number of molecules, known as single-molecule magnets, have been shown to retain a net magnetization upon removal of an applied magnetic field, similar to the behavior exhibited by classical permanent magnets.¹ This slow magnetic relaxation arises due to a uniaxial magnetic anisotropy, quantified by the axial zero-field splitting parameter (*D*), which breaks the degeneracy of the *M_S* levels comprising the spin ground state (*S*) of the molecule. The discovery of single-molecule magnets has generated much interest and excitement, as these species could find use in applications such as high-density spin-based information storage and processing,² quantum computing,³ and spintronics.⁴

With the goal of maximizing the relaxation barrier (U_{eff}) in single-molecule magnets, a tremendous research effort has focused on synthesizing molecules with large values of both *S* and *D*. However, as values of U_{eff} continue to climb, a third critical parameter must also be considered: the strength of magnetic exchange between paramagnetic centers, which is quantified by the exchange coupling constant *J*. Indeed, the separation between spin ground state and excited states is directly correlated to the magnitude of *J*. When *J* is insufficiently large, low-lying spin excited states enable fast relaxation pathways that can shortcut the overall thermal barrier. As such, the development of single-molecule magnets with large values of *J* represents an important challenge. Nevertheless, the vast majority of single-molecule magnets feature multiple paramagnetic metal centers coupled to

one another only weakly through diamagnetic bridging ligands via a superexchange mechanism. As an alternative, incorporation of a paramagnetic bridging ligand between metal centers enables strong direct metal-radical exchange and thus much larger values of *J*. Despite this potential, very few single-molecule magnets have incorporated radical bridging ligands.^{1h,5,6}

Benzoquinonoid bridging ligands offer an ideal platform for the construction of radical-bridged single-molecule magnets with strong magnetic coupling, as these ligands readily undergo redox chemistry to form both diamagnetic and paramagnetic electron-transfer isomers (see Figure 1). Indeed, a number of dinuclear complexes featuring a radical form of 1,2,4,5-tetraoxolene (^OLH₂) and its derivatives have been shown to exhibit strong metal-radical interactions,⁷ in some cases so strong that the spin ground state remains isolated from excited states even at 300 K.⁸ As an extension, a radical form of the related azophenine (^{NR}LH₂) should afford even stronger coupling, owing to the more diffuse orbitals of nitrogen compared to oxygen. In support of this hypothesis, *J* has been shown to increase by 32-fold in moving from a tetraoxolene to an azophenine bridge in Cu₂ complexes.⁹ Moreover, a value of $J = -946 \text{ cm}^{-1}$ ($\hat{H} = -2J(\hat{S}_A \cdot \hat{S}_B)$) has been calculated using DFT for a mononuclear nickel(II) bis(*o*-phenylenediamine radical) complex.¹⁰ Providing an additional advantage over tetraoxolene analogues, derivatives of ^{NR}LH₂ with bulky aryl substituents (*R*) bound to the nitrogen donors can be readily synthesized through palladium-catalyzed cross-coupling reactions, thereby enabling fine control over intermolecular metal-metal separation in complexes.¹¹ Herein, we report the synthesis and magnetic analysis of an azophenine radical-bridged Fe₂ complex that, to the best of our knowledge, exhibits by far the strongest magnetic exchange coupling yet observed in a single-molecule magnet.

Reaction of anhydrous Fe(SO₃CF₃)₂ with TPyA in MeCN, followed by treatment with a mixture of ^{NPh}LH₂ and Li[N(SiMe₃)₂], afforded a dark-brown solution.¹² Subsequent diffusion of diethyl ether vapor into this solution yielded dark-yellow, needle-shaped crystals of [(TPyA)₂Fe^{II}(^{NPh}L²⁻)](SO₃CF₃)₂ · 2 MeCN (**1**). The structure of [(TPyA)₂Fe^{II}(^{NPh}L²⁻)]²⁺ (see Figure 2, upper) consists of two crystallographically equivalent [(TPyA)Fe^{II}]²⁺ units connected by a deprotonated ^{NPh}L²⁻ bridging ligand. Each Fe^{II} center resides in a distorted octahedral coordination environment, with two cis-disposed sites occupied by neighboring nitrogen donor atoms from ^{NPh}L²⁻ and the other four bound by nitrogen atoms

Received: September 25, 2013

Published: October 28, 2013



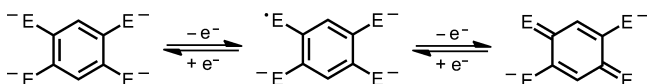


Figure 1. Redox series of deprotonated benzoquinonoid ligands. Left to right: $E-L^{4-}$, $E-L^{3-\bullet}$, $E-L^{2-}$ ($E = O$ and NR).

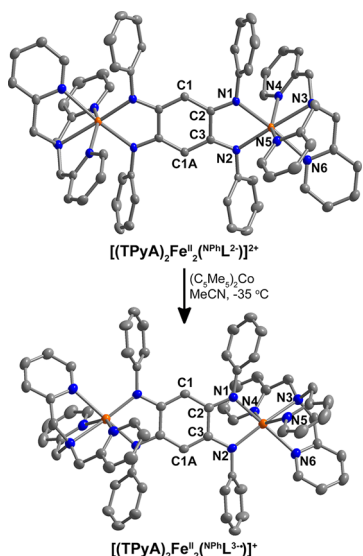


Figure 2. Reduction of $[(TPyA)_2Fe^{II}_2(N^{Ph}L^{2-})]^{2+}$ (upper) to give $[(TPyA)_2Fe^{II}_2(N^{Ph}L^{3-\bullet})]^+$ (lower). Orange, blue, and gray ellipsoids, shown at the 50% probability level, represent Fe, N, and C atoms, respectively; H atoms are omitted for clarity.

from the TPyA capping ligand. The average Fe–N distance of 2.110(3) Å is consistent with a high-spin $S = 2$ electronic configuration. The complex features an intramolecular Fe...Fe distance of 8.154(1) Å and a closest intermolecular Fe...Fe distance of 9.999(1) Å.

The cyclic voltammogram of an acetonitrile solution containing **1**, shown in Figure 3, reveals the presence of three reversible redox processes, centered at +0.32, –0.19, and –1.65 V vs $[Cp_2Fe]^{0/1+}$. Considering precedent in tetraoxolene-bridged Fe_2 complexes, we tentatively assign the first two processes to metal-centered events and the third process to a ligand-based event.^{7,8,13} Indeed, the process at –1.65 V suggests that a $[(TPyA)_2Fe_2(N^{Ph}L)]^+$ complex should be chemically accessible. Toward that end, a solution of **1** in DMF was treated at –35 °C with the strong reductant $Na(C_{10}H_8)$ ¹⁴ to give an intense blue solution.¹² Subsequent addition of diethyl ether into

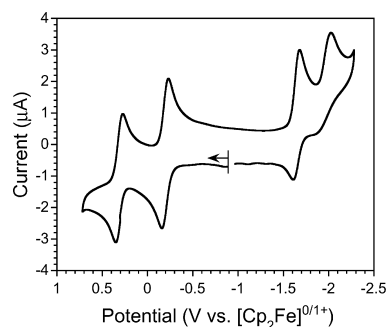


Figure 3. Cyclic voltammogram obtained for an acetonitrile solution of **1** using a platinum electrode, 50 mV/s scan rate, and 0.1 M $(Bu_4N)PF_6$ supporting electrolyte.

this solution at –35 °C afforded the one-electron-reduced compound $[(TPyA)_2Fe_2(N^{Ph}L)](SO_3CF_3) \cdot 3DMF \cdot 0.3Na \cdot (SO_3CF_3)$ (**2**) as a dark-blue microcrystalline powder in 79% yield. Alternatively, carrying out the above reaction in MeCN using the reductant $(C_5Me_5)_2Co$,¹⁵ followed by diffusion of diethyl ether vapor into the resulting solution at –35 °C, yielded a product mixture containing crystals of **1** and dark-blue, plate-shaped crystals of $[(TPyA)_2Fe_2(N^{Ph}L)](SO_3CF_3) \cdot 6MeCN$ (**2'**; see Figure 2, lower).

While the cationic complex in **2'** exhibits an overall structure similar to that in **1**, close comparison of the bond lengths in the two complexes reveals several key features (see Table 1). First, the average benzoquinone C–C distance decreases slightly by 0.9%, from 1.431(5) to 1.418(5) Å in moving from **1** to **2'**, while the average benzoquinone C–N distance increases by 2.3%, from 1.331(4) to 1.361(4) Å. These differences highlight a net increase in C–C bond order and net decrease in C–N bond order, consistent with the additional electron occupying a molecular orbital of primarily ligand character. In further support of this inference, the average Fe– N_L distance decreases by 1.8%, from 2.110(3) to 2.073(3) Å, consistent with a stronger Fe–N interaction resulting from a trianionic bridging ligand. These structural changes are similar to those previously observed for a ligand-centered reduction in a chloranilate radical-bridged Co_2 complex.^{7bc} Finally, the average Fe– N_{TPyA} distance changes only slightly, increasing from 2.233(3) to 2.249(3) Å (0.7%), supporting a ligand-centered redox event. Taken together, these observations suggest a configuration for the complex in **2** and **2'** of $[(TPyA)_2Fe^{II}_2(N^{Ph}L^{3-\bullet})]^+$. To our knowledge, **2'** represents the first structurally characterized example of a molecule incorporating a radical bridging ligand derived from azophenine.

In order to confirm the assignment of a primarily ligand-based reduction, Mössbauer spectra were collected for **1** and **2**. The Mössbauer spectrum collected on a solid sample of **1** at 77 K (see Figure 4, left) exhibits a major symmetric quadrupole doublet and a second minor doublet assigned to a small amount of Fe^{III} -containing impurity. A fit to the data provides an isomer shift of $\delta = 1.027(3)$ mm/s and a quadrupole splitting of $\Delta E_Q = 2.775(5)$ mm/s for the major doublet, consistent with two equivalent high-spin Fe^{II} ions. The spectrum of **2** exhibits a similar quadrupole doublet, with an identical isomer shift of $\delta = 1.024(4)$ mm/s and a considerably larger quadrupole splitting of $\Delta E_Q = 3.119(7)$ mm/s. The identical isomer shifts in **1** and **2** provide strong evidence that the reduction is indeed ligand centered, and the larger quadrupole splitting in **2** may stem from the change in ligand field at the Fe^{II} center associated with ligand reduction and the greater distortion from an octahedral coordination environment at iron in **2** compared to **1**. Finally, as temperature is

Table 1. Selected Bond Distances (Å) in **1** and **2'**^a

	1	2'		1	2'
C1–C2	1.410(5)	1.411(5)	Fe–N1	2.142(3)	2.103(3)
C2–C3	1.498(5)	1.461(6)	Fe–N2	2.078(2)	2.042(3)
C3–C1A	1.385(4)	1.381(4)	Fe–N_L	2.110(3)	2.073(3)
C–C	1.431(5)	1.418(5)	Fe–N3	2.297(2)	2.278(3)
N1–C2	1.318(4)	1.350(4)	Fe–N4	2.172(3)	2.314(3)
N2–C3	1.344(4)	1.372(4)	Fe–N5	2.159(3)	2.177(4)
N–C	1.331(4)	1.361(4)	Fe–N6	2.305(3)	2.226(3)
			Fe–N_{TPyA}	2.233(3)	2.249(3)

^aAverage distances are shown in bold.

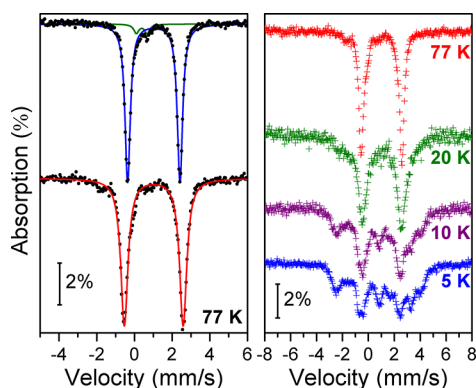


Figure 4. Left: Zero-field ^{57}Fe Mössbauer spectra for **1** (upper) and **2** (lower), collected at 77 K. Black circles correspond to experimental data, and solid lines correspond to fits of the data. Right: Variable-temperature spectra for **2**, revealing the onset of slow magnetic relaxation with lowering temperature.

decreased, the doublet in **2** undergoes spectral broadening, ultimately reaching an unresolved multiplet at 5 K (see Figure 4, right). This phenomenon indicates the onset of slow magnetic relaxation with decreasing temperature, suggesting that **2** exhibits single-molecule magnet behavior at low temperature on the Mössbauer time scale.^{16,17}

To probe and compare magnetic interactions in **1** and **2**, variable-temperature dc magnetic susceptibility data were collected for solid samples under an applied field of 1000 Oe. The resulting plot of $\chi_M T$ vs T for **1** is shown in Figure 5. At 300 K, $\chi_M T = 6.38 \text{ cm}^3 \text{ K/mol}$, corresponding to two magnetically isolated high-spin Fe^{II} centers with $g = 2.06$. As temperature is decreased, the data undergo a gradual then rapid decline, reaching a minimum value of $0.14 \text{ cm}^3 \text{ K/mol}$ at 2 K that corresponds to an $S = 0$ ground state. The decrease in $\chi_M T$ with decreasing temperature is indicative of weak antiferromagnetic superexchange coupling between high-spin Fe^{II} centers through the diamagnetic $^{\text{NPh}}\text{L}^{2-}$ ligand. To quantify this interaction, the data were fit to the Van Vleck equation according to the spin Hamiltonian $\hat{H} = -2J(\hat{S}_{\text{Fe1}} \cdot \hat{S}_{\text{Fe2}})$ to give an exchange constant of $J = -2.90(2) \text{ cm}^{-1}$.¹⁸

The plot of $\chi_M T$ vs T obtained for **2** (see Figure 5) shows a dramatically different profile than that for **1**. At 300 K, $\chi_M T = 8.84 \text{ cm}^3 \text{ K/mol}$, much higher than the value expected for two

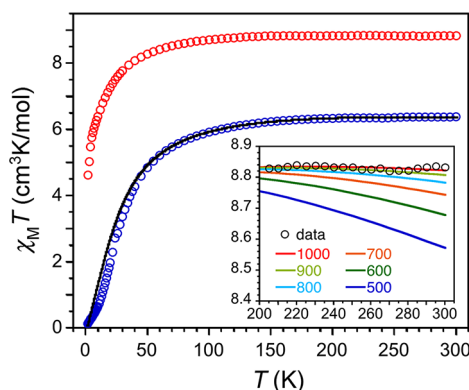


Figure 5. Variable-temperature dc magnetic susceptibility data for **1** (blue) and **2** (red), collected under an applied field of 1000 Oe. The black line corresponds to a fit of the data. Inset: Expanded view of data for **2**; lines correspond to simulations with selected values of $-J$ (cm^{-1}).

magnetically isolated $S = 2 \text{ Fe}^{\text{II}}$ centers and one $S = 1/2 \text{ } ^{\text{NPh}}\text{L}^{3-\bullet}$. Instead, this value is in agreement with an $S = 7/2$ ground state ($g = 2.12$) resulting from exceptionally strong antiferromagnetic exchange between Fe^{II} centers and $^{\text{NPh}}\text{L}^{3-\bullet}$ radical. Indeed, the invariance of $\chi_M T$ in the temperature range 130–300 K indicates that the $S = 7/2$ ground state remains well isolated from excited states even up to 300 K. While the temperature independence of $\chi_M T$ precludes a definitive quantitation of J , a lower bound of the magnitude can be estimated. The inset of Figure 5 shows an expanded view of the high-temperature data, along with simulations of the data for selected values of J according to the spin Hamiltonian $\hat{H} = -2J[\hat{S}_{\text{rad}}(\hat{S}_{\text{Fe1}} + \hat{S}_{\text{Fe2}})]$.¹⁹ These simulations provide a value of $J \leq -900 \text{ cm}^{-1}$ for **2**. This value should be regarded as an estimate, as subtle changes to the diamagnetic correction of the data and/or introduction of additional parameters to the simulation, such as zero-field splitting or intra/intermolecular $\text{Fe} \cdots \text{Fe}$ interactions, can lead to significant variation of J . Nevertheless, this estimated magnitude of J is nearly 50× larger than the $J = +19 \text{ cm}^{-1}$ observed in a chloranilate radical-bridged Fe^{II}_2 complex with ferromagnetic metal-ligand radical exchange.^{7c} Most importantly, to the best of our knowledge, this value is by far the largest ever observed in a single-molecule magnet, eclipsing the previous record of $J = -133 \text{ cm}^{-1}$, held by a recently reported nindigo radical-bridged Co^{II}_2 complex.^{6b} Finally, we note that a similar energy separation from excited states has been observed for the $S = 9/2$ ground state of a mixed-valence $[\text{Fe}_2]^{\text{V}}$ complex, however this behavior arises through a double-exchange mechanism due to electron delocalization.¹⁷

In order to assess the presence of magnetic anisotropy in **2**, low-temperature magnetization data were collected at selected dc fields (see Figure 6, lower right). The splitting of the resulting isofield curves, along with their saturation well below the expected $M = 7 \mu_B$ for an $S = 7/2$ ground state with $g = 2$, demonstrates qualitatively the presence of significant magnetic anisotropy. To quantify this effect, the data were fit using the program ANISOFIT 2.0^{20,21} to give parameters of $D = -8.4 \text{ cm}^{-1}$, $|E| = 0.6 \text{ cm}^{-1}$, and $g = 2.11$. To our knowledge, this value of D is the largest yet observed in a multinuclear single-molecule magnet, surpassing a cyano-bridged $\text{Cu}^{\text{II}}_3\text{Fe}^{\text{III}}_2$ cluster with an $S = 5/2$ ground state and $D = -5.7 \text{ cm}^{-1}$,²² and likely stems from a combination of high-anisotropy high-spin Fe^{II} centers and relatively small spin ground state. This value of D

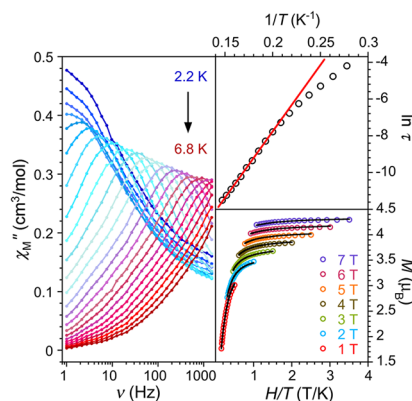


Figure 6. Left: Variable-frequency ac susceptibility data for **2**. Upper right: Arrhenius plot of relaxation time, with $U_{\text{eff}} = 50(1) \text{ cm}^{-1}$. Lower right: Low-temperature magnetization data for **2** at selected fields.

implies that **2** could behave as a single-molecule magnet with a maximum relaxation barrier of $U = (S^2 - 1/4)|D| = 101 \text{ cm}^{-1}$.

Following the observation of slow magnetic relaxation from variable-temperature Mössbauer spectroscopy and presence of a large negative D , variable-frequency ac susceptibility data under zero applied dc field were collected in order to further probe single-molecule magnet behavior. The frequency-dependent out-of-phase component (χ_M'') of the ac susceptibility (see Figure 6, left) demonstrates that **2** is indeed a single-molecule magnet. The corresponding Arrhenius plot of relaxation time (see Figure 6, upper right) exhibits a linear region at high temperature, indicative of a thermally activated relaxation process (see SI). A fit to the data in the temperature range 5.0–6.8 K provides a relaxation barrier of $U_{\text{eff}} = 50(1) \text{ cm}^{-1}$, with $\tau_0 = 2.7(2) \times 10^{-10} \text{ s}$. Considering the value of $D = -8.4 \text{ cm}^{-1}$ obtained from magnetization data, this relaxation barrier is in exact agreement with the energetic separation between ground $M_S = 7/2$ levels and first-excited $M_S = 5/2$ levels, given as $6|D| = 51 \text{ cm}^{-1}$. This observation suggests that thermally assisted quantum tunneling between $M_S = \pm 5/2$ levels acts as the dominant relaxation pathway for **2** in this temperature range. As temperature is further decreased, the data begin to deviate from linearity, denoting the presence of additional fast relaxation processes, such as quantum tunneling and/or spin–spin relaxation, that shortcut the barrier.

The foregoing results demonstrate that a radical form of azophenine can be employed as a bridging ligand to synthesize single-molecule magnets with magnetic exchange coupling of unprecedented strength. Indeed, the one-electron reduction of a $[\text{Fe}^{\text{II}}_2(\text{N}^{\text{Ph}}\text{L}^{2-})]^{2+}$ complex gives a $[\text{Fe}^{\text{II}}_2(\text{N}^{\text{Ph}}\text{L}^{3-\bullet})]^+$ complex that behaves as a single-molecule magnet with a spin ground state of $S = 7/2$ and a relaxation barrier of $U_{\text{eff}} = 50(1) \text{ cm}^{-1}$. The metal-ligand radical exchange coupling in this complex, with an estimated magnitude of $|J| \geq 900 \text{ cm}^{-1}$, is to our knowledge by far the strongest magnetic exchange yet observed in a single-molecule magnet. Work is underway to incorporate metal centers with stronger magnetic anisotropy and more radially diffuse d-orbitals to this system, append substituents onto $\text{N}^{\text{Ph}}\text{LH}_2$ in order to modulate ligand-centered redox processes, and synthesize related bridging ligands with even more diffuse donor atom orbitals.

■ ASSOCIATED CONTENT

■ Supporting Information

Experimental details and characterization data. This material is available free of charge via the Internet at <http://pubs.acs.org>.

■ AUTHOR INFORMATION

Corresponding Author

dharris@northwestern.edu

Notes

The authors declare no competing financial interest.

■ ACKNOWLEDGMENTS

Research was funded by Northwestern University, the International Institute for Nanotechnology, and the Initiative for Sustainability and Energy at Northwestern (Booster Award 10033416). We thank Prof. C. J. Chang for use of his Mössbauer spectrometer, Prof. E. A. Weiss for use of her UV/vis/near-IR spectrometer, and K. Du, J. Martinez, V. L. Weidner, and G. Yang for experimental assistance.

■ REFERENCES

- (1) (a) Caneschi, A.; Gatteschi, D.; Sessoli, R.; Barra, A. L.; Brunel, L. C.; Guillot, M. *J. Am. Chem. Soc.* **1991**, *113*, 5873. (b) Sessoli, R.; Tsai, H.-L.; Schake, A. R.; Wang, J. B.; Folting, K.; Gatteschi, D.; Christou, G.; Hendrickson, D. N. *J. Am. Chem. Soc.* **1993**, *115*, 1804. (c) Sessoli, R.; Gatteschi, D.; Caneschi, A.; Novak, M. A. *Nature* **1993**, *365*, 141. (d) Berlinguette, C. P.; Vaughn, D.; Cañada-Vilalta, C.; Galán-Mascarós, J. R.; Dunbar, K. R. *Angew. Chem., Int. Ed.* **2003**, *42*, 1523. (e) Ishikawa, N.; Sugita, M.; Ishikawa, T.; Koshihara, S.-y.; Kaizu, Y. *J. Am. Chem. Soc.* **2003**, *125*, 8694. (f) Schelter, E. J.; Prosvirin, A. V.; Dunbar, K. R. *J. Am. Chem. Soc.* **2004**, *126*, 15004. (g) Freedman, D. E.; Harman, W. H.; Harris, T. D.; Long, G. J.; Chang, C. J.; Long, J. R. *J. Am. Chem. Soc.* **2010**, *132*, 1224. (h) Rinehart, J. D.; Fang, M.; Evans, W. J.; Long, J. R. *Nat. Chem.* **2011**, *3*, 538.
- (2) (a) Bogani, L.; Wernsdorfer, W. *Nat. Mater.* **2008**, *7*, 179. (b) Ardavan, A.; Blundell, S. J. *J. Mater. Chem.* **2009**, *19*, 1754.
- (3) (a) Leuenberger, M. N.; Loss, D. *Nature* **2001**, *410*, 789. (b) Stamp, P. C. E.; Gaita-Arino, A. *J. Mater. Chem.* **2009**, *19*, 1718.
- (4) Rocha, A. R.; García-suárez, V. M.; Bailey, S. W.; Lambert, C. J.; Ferrer, J.; Sanvito, S. *Nat. Mater.* **2005**, *4*, 335.
- (5) Lanthanide complexes: (a) Poneti, G.; Bernot, K.; Bogani, L.; Caneschi, A.; Sessoli, R.; Wernsdorfer, W.; Gatteschi, D. *Chem. Commun.* **2007**, 1807. (b) Xu, J.-X.; Ma, Y.; Liao, D.-Z.; Xu, G.-F.; Tang, J.; Wang, C.; Zhou, N.; Yan, S.-P.; Cheng, P.; Li, L.-C. *Inorg. Chem.* **2009**, *48*, 8890. (c) Tian, H.-X.; Liu, R.-N.; Wang, X.-L.; Yang, P.-P.; Li, Z.-X.; Li, L.-C.; Liao, D.-Z. *Eur. J. Inorg. Chem.* **2009**, 4498. (d) Rinehart, J. D.; Fang, M.; Evans, W. J.; Long, J. R. *J. Am. Chem. Soc.* **2011**, *133*, 14236. (e) Demir, S.; Zadrozny, J. M.; Nippe, M.; Long, J. R. *J. Am. Chem. Soc.* **2012**, *134*, 18546. (f) Liu, R.; Zhang, C.; Li, L.; Liao, D.; Sutter, J.-P. *Dalton. Trans.* **2012**, *41*, 12139.
- (6) Transition-metal complexes: (a) Yoshihara, D.; Karasawa, S.; Koga, N. *J. Am. Chem. Soc.* **2008**, *130*, 10460. (b) Fortier, S.; Le Roy, J. J.; Chen, C.-H.; Vieru, V.; Murugesu, M.; Chibotaru, L. F.; Mindiola, D. J.; Caulton, K. G. *J. Am. Chem. Soc.* **2013**, *135*, 14670.
- (7) (a) Dei, A.; Gatteschi, D.; Pardi, L.; Russo, U. *Inorg. Chem.* **1991**, *30*, 2589. (b) Min, K. S.; Rheingold, A. L.; DiPasquale, A. G.; Miller, J. S. *Inorg. Chem.* **2006**, *45*, 6135. (c) Min, K. S.; DiPasquale, A. G.; Golen, J. A.; Rheingold, A. L.; Miller, J. S. *J. Am. Chem. Soc.* **2007**, *129*, 2360.
- (8) Guo, D.; McCusker, J. K. *Inorg. Chem.* **2007**, *46*, 3257.
- (9) Schweinfurth, D.; Khusniyarov, M. M.; Bubrin, D.; Hohloch, S.; Su, C.-Y.; Sarkar, B. *Inorg. Chem.* **2013**, *52*, 10332.
- (10) Chlopek, K.; Bothe, E.; Neese, F.; Weyhermüller, T.; Wieghardt, K. *Inorg. Chem.* **2006**, *45*, 6298.
- (11) (a) Wenderski, T.; Light, K. M.; Ogrin, D.; Bott, S. G.; Harlan, C. J. *Tetrahedron Lett.* **2004**, *45*, 6851. (b) Khranov, D. M.; Boydston, A. J.; Bielawski, C. W. *Org. Lett.* **2006**, *8*, 1831.
- (12) See Supporting Information for absorption spectra of **1** and **2**.
- (13) Min, K. S.; DiPasquale, A. G.; Rheingold, A. L.; White, H. S.; Miller, J. S. *J. Am. Chem. Soc.* **2009**, *131*, 6229.
- (14) Connelly, N. G.; Geiger, W. E. *Chem. Rev.* **1996**, *96*, 877.
- (15) Gennett, T.; Milner, D. F.; Weaver, M. J. *J. Phys. Chem.* **1985**, *89*, 2787.
- (16) Abbas, G.; Lan, Y.; Mereacre, V.; Wernsdorfer, W.; Clérac, R.; Buth, G.; Sougrati, M. T.; Grandjean, F.; Long, G. J.; Anson, C. E.; Powell, A. K. *Inorg. Chem.* **2009**, *48*, 9345.
- (17) Hazra, S.; Sasmal, S.; Fleck, M.; Grandjean, F.; Sougrati, M. T.; Ghosh, M.; Harris, T. D.; Bonville, P.; Long, G. J.; Mohanta, S. *J. Chem. Phys.* **2011**, *134*, 174507/1.
- (18) Boča, R. *Theoretical Foundations of Molecular Magnetism*; Elsevier: Amsterdam, 1999.
- (19) Susceptibility data were simulated using the program MAGPACK: Borrás-Almenar, J. J.; Clemente-Juan, J. M.; Coronado, E.; Tsukerblat, B. S. *J. Comput. Chem.* **2001**, *22*, 985.
- (20) Shores, M. P.; Sokol, J. J.; Long, J. R. *J. Am. Chem. Soc.* **2002**, *124*, 2279.
- (21) Data were fit using the following zero-field splitting Hamiltonian: $\hat{H} = D\hat{S}_z^2 + E(\hat{S}_x^2 - \hat{S}_y^2) + g_{\text{iso}}\mu_B\mathbf{S}\cdot\mathbf{H}$.
- (22) Wang, C.-F.; Zuo, J.-L.; Bartlett, B. M.; Song, Y.; Long, J. R.; You, X.-Z. *J. Am. Chem. Soc.* **2006**, *128*, 7162.